First science with the Keck Interferometer Nuller: high spatial resolution N-band observations of the recurrent nova RS Ophiuchi

R. K. Barry, W. C. Danchi, W. Traub, M. Kuchner, J. P. Wisniewski, et al.

R. K. Barry, W. C. Danchi, W. Traub, M. Kuchner, J. P. Wisniewski, R. Akeson, M. Colavita, M. A. Greenhouse, C. Koresko, B. Mennesson, E. Serabyn, J. L. Sokoloski, "First science with the Keck Interferometer Nuller: high spatial resolution N-band observations of the recurrent nova RS Ophiuchi," Proc. SPIE 7013, Optical and Infrared Interferometry, 70130Q (28 July 2008); doi: 10.1117/12.787085

SPIE.

Event: SPIE Astronomical Telescopes + Instrumentation, 2008, Marseille, France

First Science with the Keck Interferometer Nuller: High Spatial Resolution N-Band Observations of the Recurrent Nova RS Ophiuchi

R. K. Barry[1,2], W. C. Danchi[1], W. Traub[3], M. Kuchner[1], J. P. Wisniewski[1], R. Akeson[4], M. Colavita[4], M. A. Greenhouse[1], C. Koresko[4], B. Mennesson[3], E. Serabyn[3], J. L. Sokoloski[5]

[1]NASA, Goddard Space Flight Center, Exoplanets and Stellar Astrophysics Laboratory, Greenbelt, MD 20771
[2]Department of Physics and Astronomy, The Johns Hopkins University, Baltimore, MD 21218
[3]NASA, Jet Propulsion Laboratory, Pasadena, CA 91109
[4]California Institute of Technology, Michelson Science Center, Pasadena, CA 91125
[5]Columbia University, Columbia Astrophysics Laboratory, New York, NY 10027

ABSTRACT

We report observations of the nova RS Ophiuchi using the Keck Interferometer Nuller (KIN) taken approximately 3.8 days following the most recent outburst that occurred on 2006 February 12. The KIN operates in N-band from 8 to 12.5 μm in a nulling mode. In this mode the stellar light is suppressed by a destructive fringe, effectively enhancing the contrast of the circumstellar material located near the star. In a second, constructive-fringe mode, the instrument detects primarily the light from the central, bright source. These are the outer and inner spatial regimes, respectively. We will describe the capabilities of the KIN, including these unique modes, and outline how they were key in our discovery that dust was created between nova events. We also show how these first results from the KIN are consistent with *Spitzer* data. The KIN data show evidence of enhanced neutral atomic hydrogen emission and atomic metals including silicon located in the inner spatial regime (< 4 AU from the WD) relative to the outer regime. There are also nebular emission lines and evidence of hot silicate dust in the outer spatial region, centered at approximately ~ 17 AU from the WD, that are not found in the inner regime. The KIN and *Spitzer* data suggest that these emissions were excited in the outer spatial regime before the blast wave reached these regions. We describe the present results in terms of a new model for dust creation in recurrent novae that includes an increase in density in the plane of the orbit of the two stars created by a spiral shock wave caused by the motion of the stars through the cool wind of the red giant star. These data show the power and potential of the nulling technique which has been developed for the detection of Earth-like planets around nearby stars for the Terrestrial Planet Finder Mission and Darwin missions.

Keywords: Nulling interferometry, Keck Interferometer, recurrent novae, RS Ophiuchi, high angular resolution astronomy, dust formation, binary stars

1. INTRODUCTION

Recurrent novae (RN) are a class of classical novae (CN) which have been observed to have more than one eruption. Like CN, RN events are well-represented as surface thermonuclear runaway (TNR) on white dwarf (WD) primary stars in a binary system, but are thought to have higher mass transfer rates commensurate with their greater eruption frequency. There are two types of systems that produce recurrent novae – cataclysmic variables, in which the WD accretes from a main sequence star that orbits the WD on a time scale of hours, and symbiotic stars, in which the WD accretes from a red-giant companion that orbits that WD on a time scale of years. CN and RN produce a few specific elemental isotopes by the entrainment of metal-enriched surface layers of the WD primary during TNR reactions on the surface of the WD. Some theoretical models indicate that RN could be a type of progenitor system for supernovae.

RS Ophiuchi (RS Oph) is an RN that has undergone six recorded episodic outbursts of irregular interval since 1898.[1] The most recent outburst of the nova RS Oph was discovered at an estimated V-band magnitude

Optical and Infrared Interferometry, edited by Markus Schöller, William C. Danchi, Françoise Delplancke
Proc. of SPIE Vol. 7013, 70130Q, (2008) · 0277-786X/08/$18 · doi: 10.1117/12.787085

of 4.5 by H. Narumi of Ehime, Japan on 2006 February 12.829 UT.[2] This is 0.4 mag brighter than its historical average AAVSO V-band *peak* magnitude so it is reasonable to take Feb 12.829 (JD 2453779.329) as day zero. The distance to the RS Oph system is of importance to the interferometry community as it effects interpretation of astrometric data. There has been a good deal of disagreement in the literature with a surprisingly broad range reported, from as near as 0.4 kpc[3] to as far as 5.8 kpc.[4] Barry et al.[5] have recently undertaken a thorough review of the various techniques that have been used to derive a distance to RS Oph and obtain a distance of $1.4^{+0.6}_{-0.2}$ kpc. It is this value that we adopt for astrometric calculations in this paper.

2. THE KECK INTERFEROMETER NULLER

The KIN is designed to detect faint emission due, e.g., to an optically-thin dust envelope, at small angular distances from a bright central star.[6] Its operation differs from a more common fringe scanning optical interferometer in that a nulling stage precedes the fringe scanning stage.[6–10] The basic measurement thus remains the fringe amplitude, but both the meaning of the fringe signal in relation to the source and the processing of the fringe information differ from the normal case of a standard visibility measurement. Here we provide only a brief description of the measurement process, because this has been and will be described in depth elsewhere.[6–10]

To remove both the stellar signal and the thermal background in the MIR, a two stage interferometer has been developed. To implement this approach, each Keck telescope pupil is first split into two half-apertures, to generate a total of four collecting sub-apertures. The starlight is then nulled on the two long (85 m) parallel baselines between corresponding Keck subapertures. This generates the familiar sinusoidal fringe pattern on the sky (Fig. 1), except that the central dark fringe on the star is achromatic, and fixed on the star, to achieve deep and stable rejection of the starlight. After the nulling stage, the residual, non-nulled light making it through the first stage fringe pattern is measured by a fringe scan in a second stage combiner, the "cross-combiner", which combines the light across the Keck apertures ($\sim$ 4 m baseline). Thus, what is measured is the fringe amplitude of this "nulled source brightness distribution." This quantity is then normalized by the total signal. This is measured by moving the nullers to the constructive phase, and again scanning the cross-combiners. The basic measured quantity, the null depth, N, is then the ratio of the signals with the star in the destructive and constructive states. N is related to the classical interferometer visibility $V = (I_{max} - I_{min})/(I_{max} + I_{min})$, the modulus of the complex visibility $\hat{V}$, by a simple formula:

$$N = \frac{1 - V}{1 + V} \quad . \tag{1}$$

The long nulling baselines produce fringes spaced at about 23.5 mas at 10 μm, while the short baseline produces fringes spaced at $\sim$ 400 mas,which is similar to the size of the primary beam and is assumed to be large compared to the extent of the target object. Modulating its phase therefore modulates the transmitted flux of the entire astronomical source, as modified by the sinusoidal nuller fringes, and so the amplitude of this modulated signal gives the flux that passes through the fringe transmission pattern produced by the long baseline nullers.

3. OBSERVATIONS

We observed the nova about an hour angle of about -2.0 on the Keck Interferometer in nulling mode on 2006 Feb 16, as part of the nuller shared risk science program, with a total of three observations between day 3.831 and 3.846 post-outburst bracketed with observations of two calibrators stars, ρ Boo and χ UMa. Data were obtained at N-band (8 to 12.5 μm) through two ports of the KALI spectrograph. The Infrared Astronomical Satellite (IRAS) Low Resolution Spectrometer (LRS) spectra for the calibrator stars were flux-scaled according to the broadband IRAS 12 μm fluxes. The nova data were flux calibrated and telluric features were removed using calibrator data. These calibrators are well matched to the target flux and their size and point-symmetry are well known.

Our data analysis involves removing biases and coherently demodulating the short-baseline fringe with the long-baseline fringe tuned to alternate between constructive and destructive phases, combining the results of many measurements to improve the sensitivity, and estimating the part of the null leakage signal that is associated

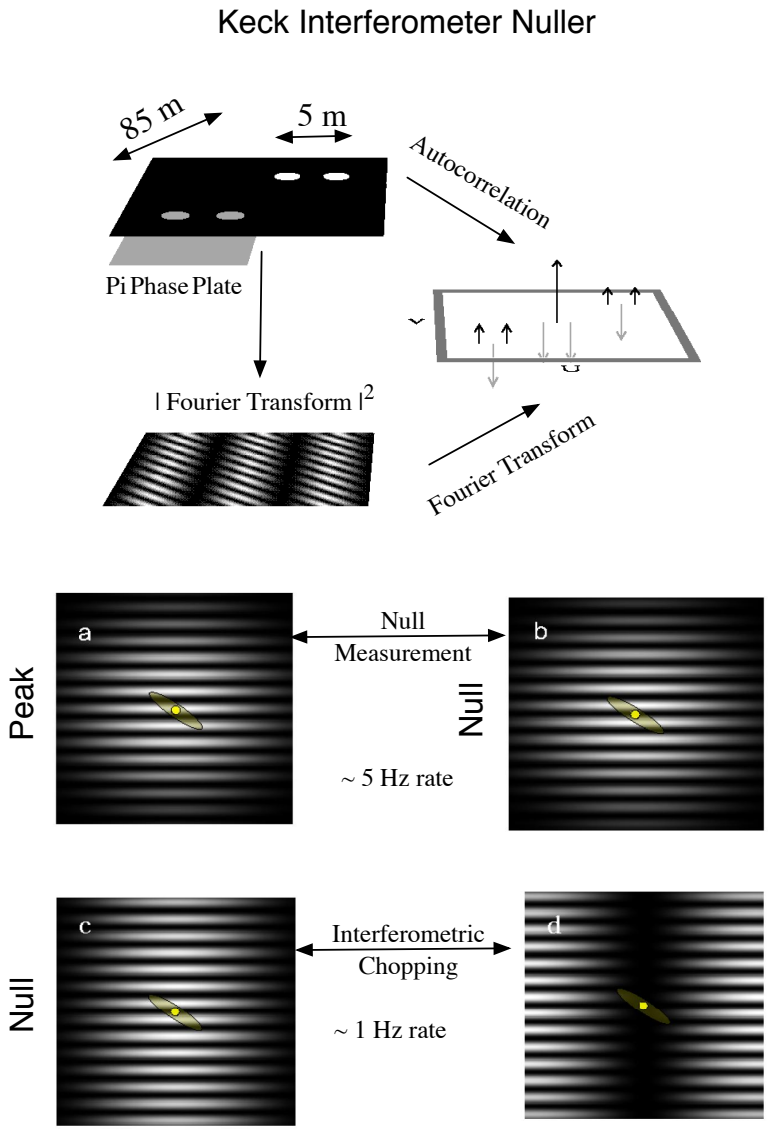

Figure 1. The upper part of this figure displays a conceptual view of the operation of the KIN system. There are two short baselines, separated by ~ 4 m, and two long baselines separated by ~ 85 m. A π phase shift is applied between the pupils on the long baseline. The autocorrelation of the four pupils is shown as well as the equivalent intensity pattern, also called the transmission pattern. Radiation passing through the white striped regions is detected by the system. Lower part of the plot displays the sequence used for the measurement process. There are two chopping sequences, (a) and (b) display the ~ 5 Hz chopping between the null and bright fringe patterns on the source using the 85 m baseline for starlight subtraction, used to measure the null response, while (c) and (d) show the ~ 5 Hz chop sequence between the two short baselines used to remove the telescope and sky backgrounds. Note that the long-baseline fringes are not to scale with the field of view in this depiction.

with the finite angular size of the central star. Data were also gated on long baseline phase and group delay. Comparison of the results of null measurements on science target and calibrator stars permits the instrumental leakage - the "system null leakage" - to be removed and the off-axis light to be measured.

Sources of noise in the measurements made by this instrument have been well described elsewhere,[11] however, we outline them here for completeness. The null leakage and intensity spectra include contributions from the astrophysical size of the object, phase and amplitude imbalances, wavefront error, beamtrain vibration, pupil polarization rotation, and pupil overlap mismatch. There are also biases, mostly eliminated by use of sky frames, in the calculated fringe quadratures, caused mainly by thermal background modulation due to residual movement of the mirrors used to shutter the combiner inputs for the long baselines. Another source of error is the KALI spectrometer channel bandpass, which is large enough to produce a significant mismatch at some wavelengths between the center wavelength and the short-baseline stroke OPD. This effect, termed warping, distorts the quadratures and is corrected by a mathematical dewarping step accomplished during calibration. There is also the effect of the partial resolution of extended structure on the long baselines which will cause the flux to be undercounted by some amount depending on the spatial extent and distribution of the emitting region. Compared to the error bars this is a rather small effect for most normal stars, and is unlikely to have much influence on the actual spectrum, though, unless the emission lines are coming from a very extended shell approaching 25 mas in angular size. We do not expect this to be the case for nova RS Oph at day 3.8.

The most important contributor to measurement noise is sky and instrument drifts between target and calibrator. Other potential sources of noise include the difference between the band center wavelength for the interferometer and that of the IRAS LRS calibrator, undercounting of stellar flux resulting from errors in the short-baseline phase tracking, and the chromaticity of the first maximum of the long-baseline fringe. None of these are significant for the following reasons. First, the calibration is based not on broadband photometry but on the IRAS LRS spectrum. Second, short-baseline tracking errors happen nearly as frequently on target observations as on calibrator observations so they should have minimal effect on overall calibrated flux. Third, the effect of chromaticity should be negligible because fringe detection is done on a per-spectral-channel basis. As a result, it is only affected by dispersion within the individual KALI spectral channels, which are about 0.3 μm in width.

Table 1. RS Ophiuchi model fitting results

Source Model	Angular Size (mas) (N band)	Radiant Flux (Jy)	Major Size (mas) (K band)	Minor size[a](mas) (K band)
Uniform Disk	6.2 ± 0.6	22.4 ± 3.9	4.9 ± 0.4	3.0 ± 0.3
Uniform Gaussian[b]	4.0 ± 0.4	22.4 ± 3.8	3.1 ± 0.2	1.9 ± 0.3
Uniform Shell[c]	5.4 ± 0.6	22.4 ± 3.8	3.7 ± 0.3	1.9 ± 0.2

[a]Sizes for continuum values at 2.3 μm after Chesneau et al.[12]
[b]Full width at half maximum.
[c]Spherical shell with thickness 1.0 mas - optically thin.

4. DATA & ANALYSIS

We developed a full mathematical solution and software suite to model the observatory and source brightness distribution. We used this suite to conduct an exhaustive grid search and to generate a monte carlo confidence interval analysis of solution spaces of these models. We explored three types of models for the source surface brightness distribution; gaussian, disk, and shell. Limited (u, v) coverage permitted only rotationally-symmetric models with two parameters - size and flux. We used χ^2 minimization to obtain the best fit models for both the inner and outer spatial regimes simultaneously. Table 1 displays size measurements, flux values, and one-σ confidence interval values. The error bars have been increased slightly beyond the χ^2 values to incorporate

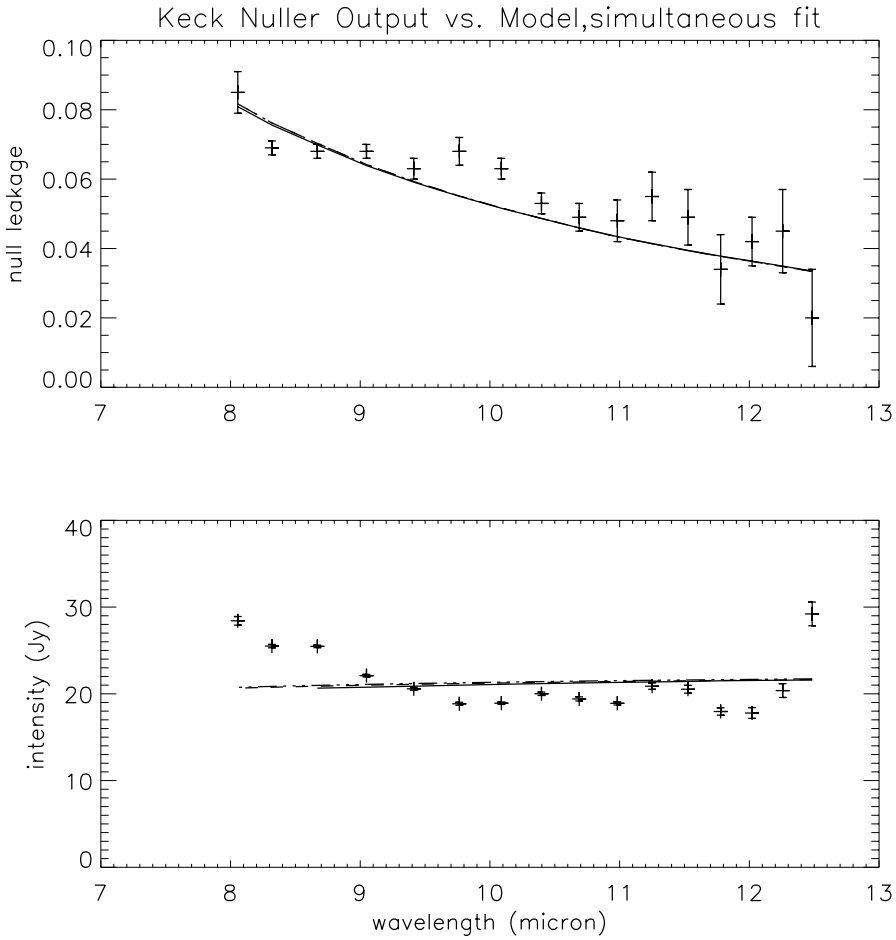

Figure 2. Plot of three best-fit continuum models against *Keck* Nuller data. All three models; disk, shell, and gaussian, that minimized χ^2 simultaneously against the null leakage and intensity spectra, lie effectively on top of one another. The top trace gives the dimensionless null leakage or interferometric observable which is the null fringe output divided by the intensity spectrum. The lower trace is the constructive fringe output or intensity spectrum. As described in the text we have removed several data points associated with emission features from the original set for the purpose of fitting the continuum.

the effect of an adopted 0.005 one-σ systematic error, which is a correlation among measurements at different wavelengths.

The measurements made with the two KALI ports are somewhat independent - the data they produce are combined for purposes of fringe tracking, but not for data reduction. The system null and the final calibrated leakage are computed separately for the two ports. The apparent inconsistency detected between the ports is the result of optical alignment drifts at the time of the measurement. In particular, the last calibrator measurement showed a sudden change in the system null for Port 1, while for all the other calibrator measurements the system nulls were stable. We therefore compared our source brightness distribution models against KALI port 2 data alone. For the best-fit models in Table 1 we used *Spitzer* spectra to identify and remove emission features centered at 8.7, 9.4, 10.4, 11.4, and 12.5 μm in the KIN inner and 8.9, 9.8, and 11.4 μm in the KIN outer spatial regime. We removed the emission feature data because our intention was to model the continuum.

Figure 2 shows two sets of $8 - 12.5$ μm spectra of RS Oph on day 3.8 post-outburst. The upper plot shows the outer spatial regime (15 to 450 mas), which is the dimensionless null leakage spectrum, i.e., the intensity of light remaining after destructive interference divided by the intensity spectrum, plotted against wavelength in

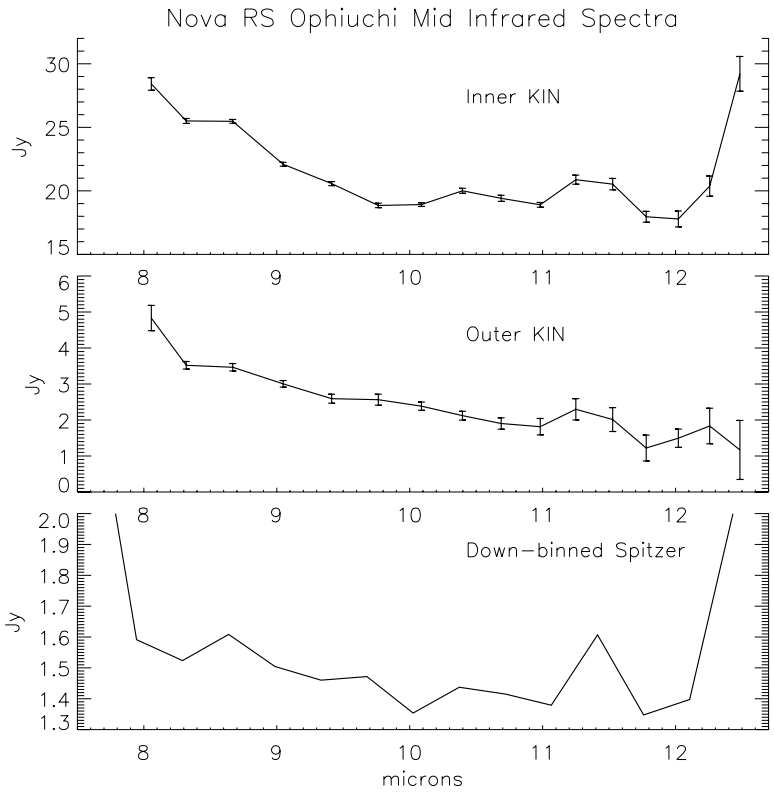

Figure 3. Plot of KIN spectra together with a *Spitzer* spectrum. Upper trace is the intensity spectrum or inner KIN spatial regime - light dominated by the inner 25 mas about the center of the source brightness distribution at mid band. The middle trace is the nulled fringe output which is the interferometric observable times the intensity spectrum multiplied by 2 (to correct for transmission through the fringe pattern for extended sources) to give the source brightness in the outer spatial regime. This is predominantly emission from material greater than about 12.5 mas (∼17 AU at 1.4 kpc) from the center of the source. The lower trace is *Spitzer* data[13] from day 63 boxcar averaged to yield approximately the same spectral resolution as the *Keck* Interferometer Nuller. None of the data were continuum normalized. Note the features between 9 and 11 μm and how the inner and outer spatial regime spectra are different from one another. Note that the Spitzer spectra have very low spatial resolution and combine the light from the entire region detected by both KIN inner and outer spatial regimes.

microns. The lower plot is the intensity spectrum, which is light principally from the inner 25 mas centered on the source brightness distribution orthogonal to the Keck Interferometer baseline direction - 38 degrees East of North. The null leakage spectrum may be broadly described as a distribution that drops monotonically with increasing wavelength overlaid with wide, emission-like features. The intensity spectrum, with an average flux density of about 22 Jy over the instrument spectral range, may be similarly described but with a continuum that has a saddle shape with a distinct rise at each end. The underlying shape curves upward for wavelengths shorter than approximately 9.7 μm and longer than 12.1 μm. Overlaid on each of these are traces representing simple models of source brightness distributions fit to the data, described above.

Figure 3 shows the inner and outer spatial regimes from the KIN data together with *Spitzer* data from day 63 from Evans et al.[14] The absolute fluxes of these data are given with a broken ordinate axis for clarity. The outer KIN spectrum flux has been multiplied by 2 to correct for the transmission through the fringe pattern for extended sources. In efforts to identify the sources of these emission features we took the high resolution *Spitzer* spectra and, using boxcar averaging, re-binned the data until it and the KIN data had equivalent resolution. The

binned *Spitzer* spectrum is quite similar in character to the KIN spectra. Importantly, the sum of the inner and outer spatial regime KIN spectra is nearly identical to the binned *Spitzer* spectrum with the exception that the absolute scale magnitude is, on day 3.8, about an order of magnitude greater than that of the *Spitzer* spectrum. This is as expected because the measured flux drops with time after the peak due to cooling and the summed inner and outer spatial regime data should very nearly reproduce the transmission of a filled aperture telescope of equivalent diameter.

The wavelength range sampled by the KALI spectrometer, 8 - 12.5 μm, covers many important discrete transitions including molecular rotation-vibration, atomic fine structure, and electronic transitions of atoms, molecules, and ions. This range also samples several important transitions in solids such as silicates found in dust and polycyclic aromatic hydrocarbons (PAHs). With the exception noted below, spectral features in the KIN data are clearly not resolved by the instrument and are often, in the associated *Spitzer* spectrum, Doppler broadened and blended. Also, because the *Spitzer* spectra were not taken contemporaneously with the KIN spectra and because of the transient nature of the RN, identification of KIN features with *Spitzer* lines is necessarily tentative.

Table 2. Continuum-normalized, Mid-infrared KIN Emission Source Identification

Center Wavelength (μm)	Spectroscopic Width (μm, FWZI)	Flux (Jy)	Attributed to
KIN Inner Spatial Regime			
8.7	8.3 - 9.1[a]	0.06[b]	H I: 10-7, FeI, Ca I[c]
9.4	8.9 - 11.1	0.02	Ca I, Si I, C I, C II
10.4	9.9 - 11.1	0.04	Mg I, Ne I, C I]
11.4	11.1 - 11.8	0.07	He I, He II
12.5	12.1 - 12.6	0.15	Huα
KIN Outer Spatial Regime			
8.9	8.3 - 9.5	0.14	H I: 10-7, [V II], Si I, Ca I][d]
9.8	9.0 - 10.7	0.24	Silicate Dust[e]
11.4	11.0 - 11.8	0.19	H I: 9 - 7, He I, He II

[a]Approximate FWZI continuum crossing points.

[b]Because *Keck* and *Spitzer* data were not taken simultaneously and because of the extreme transient nature of the RN outburst it is not possible to determine flux values for the atomic lines attributed to the KIN features. The fluxes listed should be considered the maximum bound on the flux for any one of the atomic species shown here.

[c]All atomic line emission in the KIN inner spatial regime is assumed to be emitted by a species at approximate cosmic abundance as for RN only a very moderate amount of nucleosynthesis is theorized to occur.

[d]All atomic line emission in the KIN Outer spatial regime are assumed to be predominantly of nebular abundance with some contribution from uncondensed metals.

[e]This feature is spectrally resolved and partially resolved spatially. The silicate dust feature has more than seven spectral elements across it and emits relatively strongly at a distance centered $\sim$ 17 AU from the WD. All flux is assumed to be attributable to emission by the dust.

Table 2 gives our identification of particular emission sources with the continuum-normalized spectral features in the KIN inner and outer spectra. The center wavelength of each of the broad features is listed in the first column, while the second column displays a width for each feature defined as the cutoff wavelength at the intersection of the the feature and the unity continuum line - the full-width zero intensity (FWZI) level of the feature. The flux and the one-σ uncertainty contained in that feature through measurement of the total area under it and above the unity continuum level is in the third column. The fourth column shows the particular atomic species found in the *Spitzer* spectrum with each KIN spectral feature. Because *Spitzer* lacks the spatial resolution to discriminate the inner from the outer regions of the nova and the KIN lacks the spectral resolution

to discriminate among atomic species we assumed that features in the KIN spectra would most reasonably be identified with *Spitzer* features that were in later spectra. In particular, *Spitzer* emission lines features identified with corresponding ones in KIN inner spatial regime, dominated by light originating in the close vicinity the WD, are well-represented by a cosmic distribution of atomic elements. We assumed that any condensates within the blast radius of the nova would be sublimated away and dissociated into atoms, and that any nucleosynthesis that occurred in the outer layers of the WD during TNR would negligibly impact abundances. The KIN inner spatial regime spectral features were keyed to *Spitzer* spectral features in the 4/16 and 4/26 spectra. Similarly, the KIN outer spatial regime, light predominantly from a region $\sim$ 17 AU from the WD, is keyed to the *Spitzer* spectrum taken on 9/9 by Evans et al.[15] as it is assumed that the abundances of atomic species in the latter, nebular *Spitzer* spectrum, would reasonably be representative of the environment observed by that KIN channel.

Note that our KIN data detects the faint emission from well outside of the blast radius, assuming an initial shock front velocity of 3500 km/s (Sokoloski, et al.[16]) and negligible deceleration. The radiation from this spatial region originates primarily from material around the nova that has been illuminated and warmed by photons from the nova flash and, as a result, must have existed *before* the nova event. This establishes that silicate dust, created in the vicinity of the RS Ophiuchi system some time previous to the 2006 outburst, is detected by our measurements, and is consistent with the conclusions of Evans et al.[14]

5. A PHYSICAL MODEL FOR THE NOVA

Mastrodemos & Morris[17] computed three-dimensional hydrodynamical models of morphologies of the envelopes of binaries with detached WD and RG/AGB components in general. Their purpose was to see if these models could reproduce some of the observed characteristics of axisymmetric or bipolar pre-planetary nebulae. Their study focused on a parameter space that encompassed outflow velocities from 10 to 26 km/s, circular orbits with binary separations from 3.6 to 50 AU, and binary companions having a mass range of 0.25 to 2 $M_{\odot}$. For binary separations of about 3.6 AU and mass ratios of 1.5, it was possible to generate a single spiral shock that winds 2-3 times around the binary before it dissipates at $>$ 25 times the radius of the RG star. There is a density enhancement of about a factor of 100 over the normal density in the wind in the plane of the orbit of the two stars, and an under density or evacuated region perpendicular to the plane of the orbit. Observational support for this model was found recently by Bode et al.[18] who detected a double-ring structure in HST data, which they interpreted as due to an equatorial density enhancement and Mauron & Huggins[19] who observed a spiral pattern around the AGB star AFGL 3068 both of which were consistent with the model of Mastordemos & Morris.[17] The underlying binary in AFGL 3068, a red giant and white dwarf, was discovered by Morris et al.,[20] who also determined the binary separation and hence approximate orbital period, which was consistent with expectations from the appearance of the spiral nebula pattern seen by Mauron & Huggins[19] and the model.

Figure 4 shows the proposed geometry of the nebula as viewed from a 33 degree inclination angle to the line of site to the RS Oph system based on the parameters adopted from Dobrzycka & Kenyon[21] for the system, including an orbital period of 460 days, and an inclination angle of about 33 degrees, for the epoch just prior to the nova outburst. The spiral shock model produces an archimedian spiral nebula, with the separation between adjacent windings of about 3.3 mas based on the period noted above and a wind speed from the red giant star of 20 km/s. Based on these parameters we estimate that about 17 such rings could be created between outbursts, with the overall size of the nebula of the order of 100 mas. However, there could be as few as 10 rings to as many as about 20 rings, depending on the parameters, some of which are not well known.

6. CONCLUSION

We analyzed data from the recurrent nova RS Oph for the epoch at $\sim$ 4 days post-outburst using the new KIN instrument. These data allowed us to determine the size of the emitting region around the RS Oph at wavelengths from 8-12 μm. By fitting the unique KIN inner and outer spatial regime data, we obtained an angular size of the mid-infrared continuum of 6.2, 4.0, or 5.4 mas for a disk profile, gaussian profile (FWHM), and shell profile respectively. The data show evidence of enhanced neutral atomic hydrogen emission located in the inner spatial regime relative to the outer regime. There is also evidence of a 9.7 μm silicate feature seen outside of this region, which is consistent with dust that had condensed prior to the outburst, and which has not

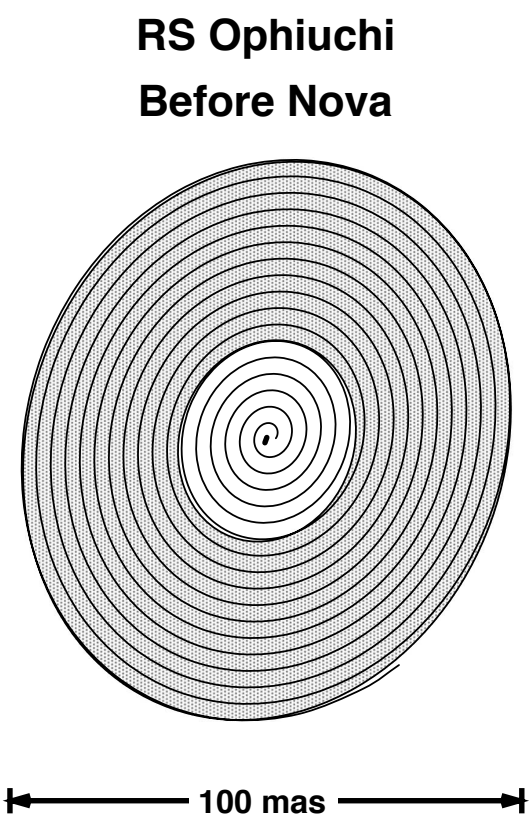

Figure 4. Proposed model of circumstellar material surrounding the binary RS Oph before the nova eruption. The interaction of the white dwarf and red giant star in the slow dense wind of the red giant star can create a spiral shock with an enhanced density in the plane of the orbit of the two stars. The overall size of the dense in-plane material is of the order of 100 mas if RS Oph is at a distance of 1400 pc and the wind speed is about 20 km/s.

yet been disturbed by the blast wave from the nova. Our analysis of the observations, including the new ones presented in this paper, are most consistent with a new model for dust production in symbiotic RN, in which spiral shock waves associated with the motion of the two stars through the cool wind from the red giant create density enhancements within the plane of their orbital motion.

7. ACKNOWLEDGMENTS

We are grateful to the National Aeronautics and Space Administration, Jet Propulsion Laboratory, the California Association for Research in Astronomy, the Harvard-Smithsonian Center for Astrophysics (including SAO grant G06-7022A to JLS), and to the National Aeronautics and Space Administration, Goddard Space Flight Center for support of this research. The data presented herein were obtained at the W.M. Keck Observatory, which is operated as a scientific partnership among the California Institute of Technology, the University of California and the National Aeronautics and Space Administration. The Observatory was made possible by the generous financial support of the W.M. Keck Foundation. JPW acknowledges support provided by an NPP Fellowship (NNH06CC03B) at NASA Goddard Space Flight Center. This work has made use of services produced by the Michelson Science Center at the California Institute of Technology.

REFERENCES

[1] Barry, R. K., Danchi, W. C., Traub, W. A., Sokoloski, J. L., Wisniewski, J. P., Serabyn, E., Kuchner, M., Akeson, R., and 33 authors, 2008, ApJ, 677, 1253

[2] Narumi, H., Hirosawa, K., Kanai, K., Renz, W., Pereira, A.,Nakano, S., Nakamura, Y., & Pojmanski, G. 2006, IAUC, 8671, 2
[3] Hachisu, I., & Kato, M., 2001, ApJ, 558, 323
[4] Pottasch, S. R., 1967, BAIN, 19, 227
[5] Barry, R.K., Mukai, K., Sokoloski, J. L., Danchi, W. C., Hachisu, I., Evans, A., Gehrz, R., & Mikolajewska, J., 2008, in RS Ophiuchi (2006) and the recurrent nova phenomenon, eds A. Evans, M. F. Bode, T. J. O'Brien, Astronomical Society of the Pacific Conference Series, accepted
[6] Serabyn, E., Colavita, M.M. & Beichman, C.A. 2000, in Thermal Emission Spectroscopy and Analysis of Dust, Disks, and Regoliths, ASP Conf. Ser. Vol. 196, eds. M.L. Sitko, A.L. Sprague & D.K. Lynch, p. 357.
[7] Serabyn, E. et al. 2004, in SPIE Vol. 5491, New Frontiers in Stellar Interferometry, ed. W.A. Traub, 136.
[8] Serabyn, E. et al. 2005, in SPIE Vol. 5905, Techniques and Instrumentation for Detection of Exoplanets II, ed. D.R. Coulter, 5905OT-1.
[9] Serabyn, E. et al. 2006, Proc. SPIE 6268, Advances in Stellar Interferometry, eds. J.D. Monnier, M. Scholler and W.C. Danchi, 626815.
[10] Colavita, M.M. Serabyn, G. Wizinowich, P.L. & Akeson, R.L. 2006, in Advances in Stellar Interferometry, eds. J.D. Monnier, M. Scholler and W.C. Danchi, Proc. SPIE 6268, 626803
[11] Koresko, C., Colavita, M., Serabyn, E., Booth, A., & Garcia, J., 2006, Proc. SPIE, 6268, 626816-1
[12] Chesneau, O., Nardetto, N., Millour, F., Hummel, C., Domiciano de Souza, A., Bonneau, D., Vannier, M., Rantakyro, F., Spang, A., Malbet, F., Mourard, D., Bode, M. F., OBrien, T. J., Skinner, G., Petrov, R. G., Stee, P., Tatulli, E., & Vakili, F., 2007, A&A, 464, 119
[13] Evans, A., Woodward, C.E., Helton, A., Gehrz, R. D., Lynch, D. K., Rudy, R. J., Russell, R. W., Bode, M. F., Kerr, T., Yang, B., Matsuoka, Y., Tsuzuki, Y., Eyres, S. P. S., Geballe, T. R., O'Brien, T. J., Davis, R. J., Starrfield, S. G., Ness, J.-U., Drake, J., Osborne, J. P., Page, K. L., Schwarz, G., & Krautter, J., 2007, ApJ, 663L, 29E
[14] Evans, A., Woodward, C., Helton, A., van Loon, J. Th., Barry, R. K., Bode, M. F., et al., 2007, ApJ, 671, L157
[15] Evans, A., Woodward, C., Helton, A., van Loon, J. Th., Barry, R. K., Bode, M. F., et al., 2007, ApJ, 671, L157
[16] Sokoloski, J., et al., 2006, Nature, 442, 276
[17] Mastrodemos, N., & Morris, M., 1999, ApJ, 523, 357
[18] Bode, M. F., Harman, D. J., O'Brien, T. J., Bond, H. E., Starrfield, S., Darnley M. J., Evans, A., & Eyres, S. P. S., 2007, ApJ, 665, L63
[19] Mauron, N., & Huggins, P.J., 2006, A&A, 452, 257
[20] Morris, M., Sahai, R., Matthews, K., Cheng, J., Lu, J., Claussen, M., & Sanchez-Contreras, C., 2006, in Planetary Nebulae in our Galaxy and Beyond, Proceedings of IAU Symposium No. 234, M. J. Barlow & R. H. Mendez, eds., 469.
[21] Dobrzycka, D., & Kenyon, S. J., 1994, ApJ, 108, 2259